Research Article

AI-Powered Copilots for Precision Diagnosis and Surgical Assessment of Histological Growth Patterns in Resectable Colorectal Liver Metastases: A Prospective Study

Ruichong Lin[1,2#], Yongjian Chen[3#], Yanchun Li[4#], Yujie Tan[4,1#], Chao Wang[5#], Zehua Wang[1#], Mengyang Sun[1], Lin Wang[6], Yufei Wu[4], Weidong Pan[5], Zongyan Li[5], Zuxiao Chen[5], Zheyu Zheng[5], Xiaoming Huang[5], Lei Zhang[5], Sunjing Song[7], Zaopeng He[7], Nannan Li[1*], Yunfang Yu[1,4*] and Dawei Zhang[5*]*

Abstract

Background: Colorectal cancer (CRC) is a leading cause of mortality in China, with metastasis significantly contributing to poor outcomes. Histopathological growth patterns (HGPs) in colorectal liver metastasis (CRLM) provide vital prognostic insights, yet the limited number of pathologists highlights the need for auxiliary diagnostic tools. Recent advancements in artificial intelligence (AI) have demonstrated potential in enhancing diagnostic precision, prompting the development of specialized AI models like COFFEE to improve the classification and management of HGPs in CRLM patients.

[1]Faculty of Innovation Engineering, Institute for AI in Medicine, Faculty of Medicine, Faculty of Humanities and Arts, Macau University of Science and Technology, Taipa, Macao, China

[2]Department of Computer and Information Engineering, Guangzhou Huali College, Guangzhou, China

[3]Department of Medicine Solna, Center for Molecular Medicine, Karolinska Institutet, Stockholm, Sweden

[4]Department of Medical Oncology, Department of Pathology, Sun Yat-sen Memorial Hospital, Sun Yat-sen University, Guangzhou, China

[5]Department of Pancreatic Hepatobiliary Surgery, Department of Pathology, Department of Breast Surgery, The Sixth Affiliated Hospital, Sun Yat-Sen University, Guangzhou, China

[6]Department of Physic, Faulty of Science, Hong Kong Baptist University, Koowlong tong, HongKong, China

[7]Foshan Shunde Lecong Hospital, Foshan, China

[#]Contributed equally

[*]Corresponding author: Zaopeng He, Foshan Shunde Lecong Hospital, Foshan, China;

Nannan Li, Faculty of Innovation Engineering, Institute for AI in Medicine, Faculty of Medicine, Faculty of Humanities and Arts, Macau University of Science and Technology, Taipa, Macao, China;

Yunfang Yu, Faculty of Innovation Engineering, Institute for AI in Medicine, Faculty of Medicine, Faculty of Humanities and Arts, Macau University of Science and Technology, Taipa, Macao;

Department of Medical Oncology, Department of Pathology, Sun Yat-sen Memorial Hospital, Sun Yat-sen University, Guangzhou, China; E-mail: yuyf9@mail.sysu.edu.cn

Dawei Zhang, Department of Pancreatic Hepatobiliary Surgery, Department of Pathology, Department of Breast Surgery, The Sixth Affiliated Hospital, Sun Yat-Sen University, Guangzhou, China;

Published Online: 24 January, 2025

DOI: 10.31487/j.ANN.2024.11.05

Methods: This study developed a transformer-based deep learning model, COFFEE, for the precise classification of colorectal cancer subtypes using whole slide images (WSIs) from 514 patients diagnosed with colorectal cancer liver metastasis. The model was pre-trained using DINO on 1,442 WSIs from the TCGA-COAD cohort, utilizing a vision transformer (ViT) architecture to extract 384-dimensional feature vectors from 256 × 256 pixel patches. The proposed model integrates a transformer-based multiple instance learning (TransMIL) framework, which effectively aggregates spatial and morphological information through multi-head self-attention and pyramid position encoding generator (PPEG) modules. This design enables efficient handling of large instance sequences within WSIs, allowing for accurate binary and four-class classification. The model was validated on 972 WSIs from a recent dataset, demonstrating its robustness and clinical applicability.

Results: A total of 431 patients were included in three cohorts: training (n=297), testing (n=104), and prospective (n=30). Desmoplastic tumors were associated with longer overall survival (OS, 53.6 vs. 31.9 months, p=0.002) and progression-free survival (PFS, 25.2 vs. 10.7 months, p<0.001) compared to non-desmoplastic tumors. The COFFEE binary classification model achieved high predictive performance with AUC values of 0.961 in the training, 0.935 in the testing, and 1.000 in the prospective cohort. The four-class model also showed strong performance, with AUCs of 0.961 and 0.966 in the training and testing cohorts, and 0.985 in the prospective cohort. AI-assisted models helped junior pathologists achieve an accuracy of 94.7% (vs. 85.9%) and reduced diagnostic time by 36%, improving both accuracy and speed.

Conclusion: This study developed the first AI model for HGP classification in colorectal cancer liver metastasis, achieving high accuracy in both binary classification and four-class classification models. The model demonstrated potential for improving diagnostic precision and guiding post-surgery treatment strategies, with AI-assisted pathologists surpassing traditional methods in a prospective randomized trial.

Keywords: *Colorectal liver metastasis (CRLM), histopathological growth patterns (HGPs), artificial intelligence (AI) in diagnosis, vision transformer (ViT), desmoplastic classification*

(ANNSURG 2024; 201: 1-13)

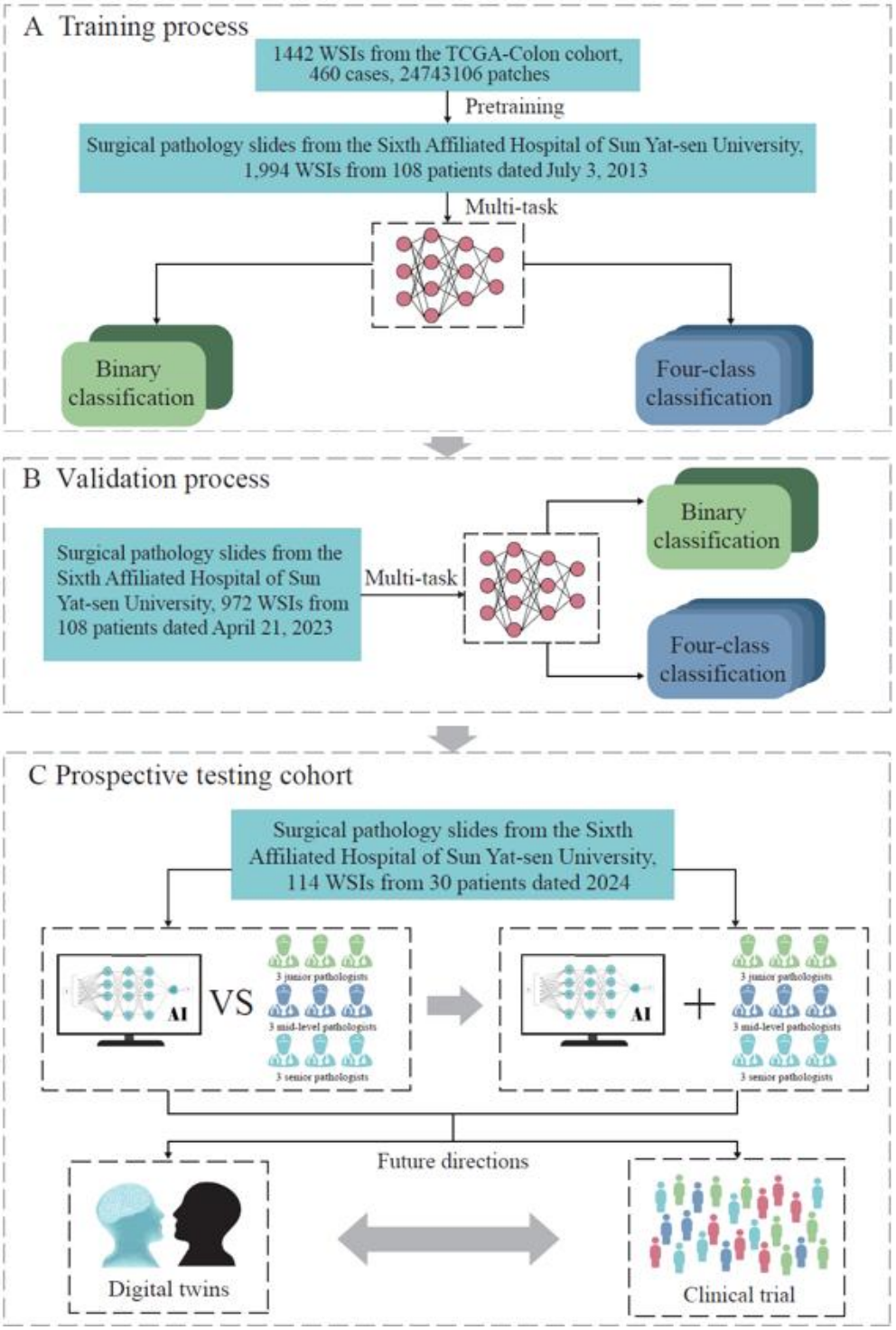

FIGURE 2. Illustrates the application of an advanced artificial intelligence (AI) system in assisting the clinical classification of colorectal cancer liver metastasis (CRLM) based on histopathological analysis.

A) Training process: The model was pre-trained using the TCGA-Colon cohort, followed by further training with CRLM pathology slides from SAHSYSU (2013). The model demonstrated high accuracy and speed in binary and four-class classifications, aiding pathologists with rapid diagnostic results. **B)** Testing process: The COFFEE model was tested using 2023 CRLM pathology slides from SAHSYSU. Results from data collected a decade earlier confirmed the model's reliability in clinical practice. **C)** Prospective validation cohort: In 2024, pathology slides from

30 CRLM patients were used to evaluate the COFFEE model. The left framework compared the model's performance with that of junior, intermediate, and senior pathologists in binary and four-class classifications. The right framework assessed the impact of COFFEE model assistance on pathologist performance. The results showed that the COFFEE model achieved comparable accuracy to senior pathologists with faster classification speeds, significantly enhancing the accuracy and speed of pathologists in WSI-based CRLM classification. The model also has potential for future applications in digital twin technology and clinical trials.

TABLE 1. Baseline characteristics of training, testing, and prospective cohorts.

Variable	Training cohort (N = 297)	Testing cohort (N = 104)	Prospective cohort (N = 30)
Follow up, months (median, IQR)	23 (16, 38)	11 (8, 17)	6 (5, 7)
Gender			
Female	89 (30%)	42 (40%)	14 (47%)
Male	208 (70%)	62 (60%)	16 (53%)
Age, years (median, IQR)	58 (49, 65)	58 (51, 65)	56 (42, 61)
<60	167 (56%)	59 (57%)	17 (57%)
≥60	130 (44%)	45 (43%)	13 (43%)
CEA (U/ml, [median, IQR])	7 (3, 21)	7 (4, 21)	5 (3, 19)
CA199 (U/ml, [median, IQR])	12 (5, 59)	15 (5, 75)	9 (5, 37)
CA125 (U/ml, [median, IQR])	13 (9, 19)	12 (8, 19)	14 (10, 21)
Number of liver segments involved			
≤2	169 (57%)	48 (46%)	14 (47%)
3	56 (19%)	19 (18%)	3 (10%)
4	37 (12%)	12 (12%)	5 (17%)
≥5	35 (12%)	25 (24%)	8 (27%)
Number of liver metastases			
≤2	175 (59%)	53 (51%)	14 (47%)
3 - 5	70 (24%)	23 (22%)	5 (17%)
≥5	52 (18%)	28 (27%)	11 (37%)
Maximum size of liver metastases exceeds 3cm			
No	148 (50%)	65 (63%)	23 (77%)
Yes	149 (50%)	39 (38%)	7 (23%)
Preoperative chemotherapy			
No	142 (48%)	38 (37%)	7 (23%)
Yes	155 (52%)	66 (63%)	23 (77%)
Tumor site			
Left colon	244 (82%)	68 (65%)	26 (87%)
Right colon	53 (18%)	36 (35%)	4 (13%)
Pathological T stage			
T0	6 (2.0%)	0 (0%)	1 (3.3%)
T1	2 (0.7%)	0 (0%)	0 (0%)
T2	27 (9.1%)	8 (7.7%)	3 (10%)
T3	197 (66%)	73 (70%)	24 (80%)

T4	65 (22%)	23 (22%)	2 (6.7%)
Pathological N stage			
N0	102 (34%)	43 (42%)	13 (43%)
N1	146 (49%)	38 (37%)	13 (43%)
N2	48 (16%)	22 (21%)	4 (13%)
Pathological type			
Infiltrating	45 (15%)	20 (19%)	3 (10%)
Mass	89 (30%)	23 (22%)	6 (20%)
Ulcerative	163 (55%)	61 (59%)	21 (70%)
Differentiation			
Highly	39 (13%)	9 (8.7%)	2 (6.7%)
Moderately	215 (72%)	80 (77%)	27 (90%)
Poorly	43 (14%)	15 (14%)	1 (3.3%)
Intravascular tumor thrombus			
No	204 (69%)	64 (62%)	22 (73%)
Yes	93 (31%)	40 (38%)	8 (27%)
Ki67	50 (30, 70)	60 (40, 70)	70 (40, 70)
HER2 stage*			
0	213 (72%)	80 (78%)	22 (73%)
1+	49 (16%)	18 (17%)	6 (20%)
2+	23 (7.7%)	3 (2.9%)	2 (6.7%)
3+	12 (4.0%)	2 (1.9%)	0 (0%)
Genes mutation			
Wild type	145 (49%)	62 (62%)	17 (57%)
Mutation**	152 (51%)	38 (38%)	13 (43%)
BRAF mutation	23 (7.6%)	3 (2.9%)	2 (6.3%)
EGFR mutation	1 (0.3%)	1 (1.0%)	0 (0%)
KRAS mutation	71 (24%)	25 (24%)	11 (34%)
NRAS mutation	28 (9.3%)	1 (1.0%)	0 (0%)
PIK3CA mutation	34 (11%)	11 (11%)	2 (6.3%)
UGT1A1 mutation	0 (0%)	1 (1.0%)	0 (0%)

HER2: Human Epidermal growth factor receptor 2; CEA: Carcinoembryonic Antigen; CA199: Carbohydrate Antigen 19-9; CA125: Cancer Antigen 125; IQR: Interquartile Range.

* 0 (Negative): No membrane positivity, 0% proportion; interpreted as negative;

1+ (Weakly Positive): Weak membrane positivity, ≤10% proportion; interpreted as negative;

2+ (Equivocal): Moderate to strong membrane positivity, 10-50% or ≥50% proportion; interpreted as equivocal, FISH testing recommended;

3+ (Positive): Strong membrane positivity, ≥50% proportion; interpreted as positive.

** Eleven patients have double gene mutations.

TABLE 2. Pathological classifications in training testing and, prospective cohorts.

Variable	Training cohort (N = 297)	Testing cohort (N = 104)	Prospective cohort (N = 30)
Binary pathological classification			
Desmoplastic	98 (33%)	39 (38%)	7 (23%)
Non-desmoplastic	199 (67%)	65 (63%)	23 (77%)
Four-class pathological classification			
Desmoplastic	223 (75%)	75 (72%)	20 (67%)
Replacement	42 (14%)	12 (12%)	7 (23%)
Pushing	21 (7.1%)	11 (11%)	0 (0%)
Mixed	11 (3.7%)	6 (5.8%)	3 (10%)

TABLE 3. Clinicopathological characteristics of the training cohort based on binary pathological classification.

Variable	Desmoplastic N = 98	Non-desmoplastic N = 199	p-value
Gender			0.2
Female	25 (26%)	64 (32%)	
Male	73 (74%)	135 (68%)	
Age, years (median, IQR)	58 (47, 64)	58 (49, 66)	0.4
<60	59 (60%)	108 (54%)	0.3
≥60	39 (40%)	91 (46%)	
CEA (U/ml, [median, IQR])	6 (3, 12)	9 (4, 29)	0.002
CA199 (U/ml, [median, IQR])	8 (4, 25)	18 (6, 90)	0.002
CA125 (U/ml, [median, IQR])	12 (9, 21)	13 (8, 19)	0.6
Number of liver segments involved			0.7
≤2	57 (58%)	112 (56%)	
3	21 (21%)	35 (18%)	
4	10 (10%)	27 (14%)	
≥5	10 (10%)	25 (13%)	
Number of liver metastases			0.6
≤2	61 (62%)	114 (57%)	
3 - 5	20 (20%)	50 (25%)	
≥5	17 (17%)	35 (18%)	
Maximum size of liver metastases exceeds 3cm			0.7
No	47 (48%)	101 (51%)	
Yes	51 (52%)	98 (49%)	
Preoperative chemotherapy			0.8
No	46 (47%)	96 (48%)	
Yes	52 (53%)	103 (52%)	
Tumor site			0.036
Left colon	74 (76%)	170 (85%)	
Right colon	24 (24%)	29 (15%)	
Pathological T stage			0.3

T0	4 (4.1%)	2 (1.0%)	
T1	0 (0%)	2 (1.0%)	
T2	11 (11%)	16 (8.0%)	
T3	63 (64%)	134 (67%)	
T4	20 (20%)	45 (23%)	
Pathological N stage			0.061
N0	42 (43%)	60 (30%)	
N1	45 (46%)	101 (51%)	
N2	11 (11%)	37 (19%)	
Pathological type			0.2
Infiltrating	18 (18%)	27 (14%)	
Mass	33 (34%)	56 (28%)	
Ulcerative	47 (48%)	116 (58%)	
Differentiation			0.4
Highly	16 (16%)	23 (12%)	
Moderately	70 (71%)	145 (73%)	
Poorly	12 (12%)	31 (16%)	
Intravascular tumor thrombus			0.9
No	68 (69%)	136 (68%)	
Yes	30 (31%)	63 (32%)	
Ki67	50 (30, 70)	50 (30, 70)	0.6
HER2 stage*			0.6
0	71 (72%)	142 (71%)	
1+	13 (13%)	36 (18%)	
2+	9 (9.2%)	14 (7.0%)	
3+	5 (5.1%)	7 (3.5%)	
Gene mutation			0.4
Wild type	51 (52%)	94 (47%)	
Mutation**	47 (48%)	105 (53%)	
BRAF mutation	9 (9.2%)	14 (6.9%)	
EGFR mutation	1 (1.0%)	0 (0%)	
KRAS mutation	20 (20%)	51 (25%)	
NRAS mutation	8 (8.2%)	20 (9.8%)	
PIK3CA mutation	9 (9.2%)	25 (12%)	
Median OS, months (95% CI)	53.6 (45.5-NA)	31.9 (27.8-45.1)	0.002
Median PFS, months (95% CI)	25.2 (18.10-38.3)	10.7 (8.07-13.6)	<0.001

HER2: Human Epidermal Growth Factor Receptor 2; CEA: Carcinoembryonic Antigen; CA199: Carbohydrate Antigen 19-9; CA125: Cancer Antigen 125; IQR: Interquartile Range; OS: overall survival; PFS: Progression-Free Survival.

* 0 (Negative): No membrane positivity, 0% proportion; interpreted as negative;

1+ (Weakly Positive): Weak membrane positivity, ≤10% proportion; interpreted as negative;

2+ (Equivocal): Moderate to strong membrane positivity, 10-50% or ≥50% proportion; interpreted as equivocal, FISH testing recommended;

3+ (Positive): Strong membrane positivity, ≥50% proportion; interpreted as positive.

** Five patients have double gene mutations.

TABLE 4. Clinicopathological characteristics of the training cohort based on four-class pathological classification.

Variable	Desmoplastic N = 223	Replacement N = 42	Pushing N = 21	Mixed N = 11	p-value
Gender					0.2
Female	62 (28%)	15 (36%)	10 (48%)	2 (18%)	
Male	161 (72%)	27 (64%)	11 (52%)	9 (82%)	
Age, years (median, IQR)	58 (50, 66)	54 (47, 64)	61 (56, 66)	60 (44, 67)	0.4
<60	127 (57%)	26 (62%)	9 (43%)	5 (45%)	0.4
≥60	96 (43%)	16 (38%)	12 (57%)	6 (55%)	
CEA (U/ml, [median, IQR])	6 (3, 19)	12 (5, 38)	10 (4, 41)	18 (9, 98)	0.006
CA199 (U/ml, [median, IQR])	10 (5, 38)	40 (9, 147)	15 (5, 171)	38 (9, 255)	0.008
CA125 (U/ml, [median, IQR])	12 (9, 19)	14 (9, 19)	12 (9, 17)	17 (9, 24)	0.6
Number of liver segments involved					0.94
≤2	126 (57%)	23 (55%)	12 (57%)	8 (73%)	
3	43 (19%)	9 (21%)	3 (14%)	1 (9.1%)	
4	29 (13%)	5 (12%)	3 (14%)	0 (0%)	
≥5	25 (11%)	5 (12%)	3 (14%)	2 (18%)	
Number of liver metastases					0.8
≤2	132 (59%)	24 (57%)	13 (62%)	6 (55%)	
3 - 5	55 (25%)	8 (19%)	5 (24%)	2 (18%)	
≥5	36 (16%)	10 (24%)	3 (14%)	3 (27%)	
Maximum size of liver metastases exceeds 3cm					0.6
No	107 (48%)	24 (57%)	12 (57%)	5 (45%)	
Yes	116 (52%)	18 (43%)	9 (43%)	6 (55%)	
Preoperative chemotherapy					0.6
No	108 (48%)	18 (43%)	12 (57%)	4 (36%)	
Yes	115 (52%)	24 (57%)	9 (43%)	7 (64%)	
Tumor site					0.4
Left colon	179 (80%)	38 (90%)	17 (81%)	10 (91%)	
Right colon	44 (20%)	4 (9.5%)	4 (19%)	1 (9.1%)	
Pathological T stage					0.99
T0	5 (2.2%)	1 (2.4%)	0 (0%)	0 (0%)	
T1	1 (0.4%)	1 (2.4%)	0 (0%)	0 (0%)	
T2	21 (9.4%)	3 (7.1%)	2 (9.5%)	1 (9.1%)	
T3	148 (66%)	27 (64%)	15 (71%)	7 (64%)	
T4	48 (22%)	10 (24%)	4 (19%)	3 (27%)	
Pathological N stage					0.3
N0	80 (36%)	11 (26%)	8 (38%)	3 (27%)	
N1	108 (49%)	23 (55%)	7 (33%)	8 (73%)	
N2	34 (15%)	8 (19%)	6 (29%)	0 (0%)	
Pathological type					0.12
Infiltrating	32 (14%)	5 (12%)	4 (19%)	4 (36%)	
Mass	75 (34%)	9 (21%)	3 (14%)	2 (18%)	
Ulcerative	116 (52%)	28 (67%)	14 (67%)	5 (45%)	

Differentiation					0.5
Highly	31 (14%)	5 (12%)	3 (14%)	0 (0%)	
Moderately	162 (73%)	30 (71%)	16 (76%)	7 (64%)	
Poorly	30 (13%)	7 (17%)	2 (9.5%)	4 (36%)	
Intravascular tumor thrombus					0.6
No	153 (69%)	27 (64%)	17 (81%)	7 (64%)	
Yes	70 (31%)	15 (36%)	4 (19%)	4 (36%)	
Ki67	50 (30, 70)	50 (30, 70)	40 (30, 70)	40 (20, 70)	0.7
HER2 stage*					0.019
0	161 (72%)	32 (76%)	15 (71%)	5 (45%)	
1+	37 (17%)	7 (17%)	3 (14%)	2 (18%)	
2+	16 (7.2%)	3 (7.1%)	3 (14%)	1 (9.1%)	
3+	9 (4.0%)	0 (0%)	0 (0%)	3 (27%)	
Gene mutation					0.6
Wild type	106 (48%)	23 (55%)	12 (57%)	4 (36%)	
Mutation**	117 (52%)	19 (45%)	9 (43%)	7 (64%)	
BRAF mutation	17 (7.5%)	6 (14%)	0 (0%)	0 (0%)	
EGFR mutation	1 (0.4%)	0 (0%)	0 (0%)	0 (0%)	
KRAS mutation	54 (24%)	7 (16%)	6 (29%)	4 (36%)	
NRAS mutation	22 (9.7%)	4 (9.3%)	2 (9.5%)	0 (0%)	
PIK3CA mutation	27 (12%)	3 (7.0%)	1 (4.8%)	3 (27%)	
Median OS, months (95% CI)	51.0 (37.9-73.7)	26.4 (22.1-NA)	58.3 (28.3-NA)	20.0 (18.2-NA)	0.033
Median PFS, months (95% CI)	17.38 (14.72-20.9)	7.98 (5.48-12.2)	12.20 (5.15-34.2)	6.82 (5.21-NA)	<0.001

HER2: Human Epidermal Growth Factor Receptor 2; CEA: Carcinoembryonic Antigen; CA199: Carbohydrate Antigen 19-9; CA125: Cancer Antigen 125; IQR: Interquartile Range; OS: Overall Survival; PFS: Progression-Free Survival.

* 0 (Negative): No membrane positivity, 0% proportion; interpreted as negative;

1+ (Weakly Positive): Weak membrane positivity, ≤10% proportion; interpreted as negative;

2+ (Equivocal): Moderate to strong membrane positivity, 10-50% or ≥50% proportion; interpreted as equivocal, FISH testing recommended;

3+ (Positive): Strong membrane positivity, ≥50% proportion; interpreted as positive.

** Five patients have double gene mutations.

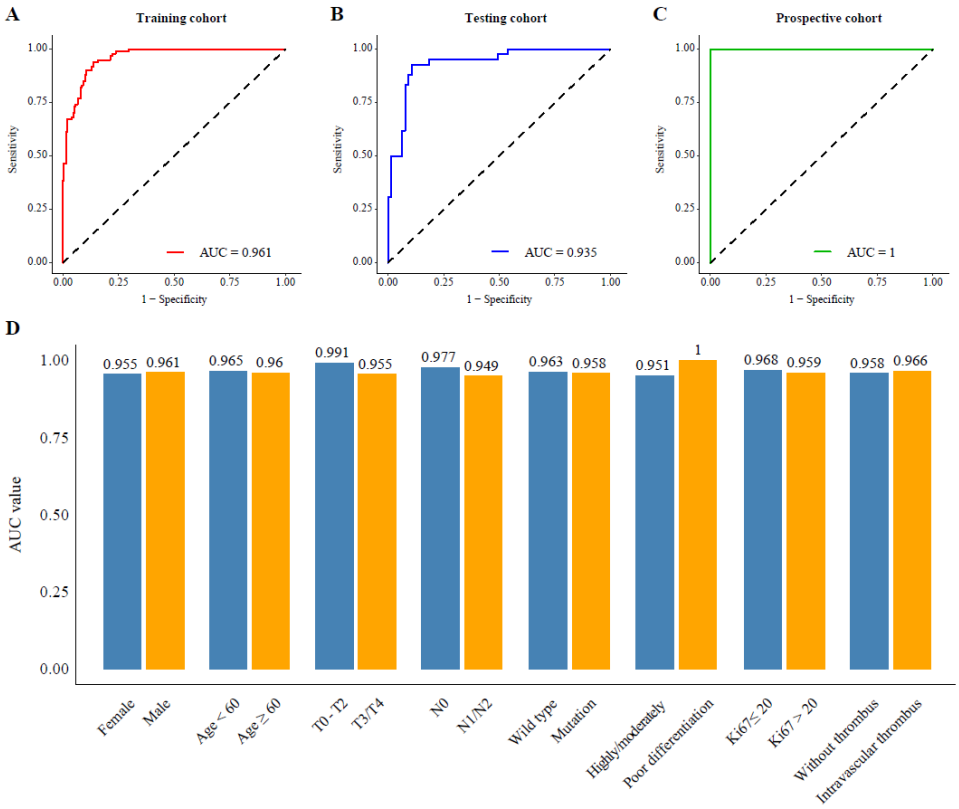

FIGURE 3. Binary Pathological Classification Prediction Performance. Performance in **A)** the training cohort, **B)** the testing cohort, and **C)** the prospective cohort, **D)** subgroup analysis of AUC values.

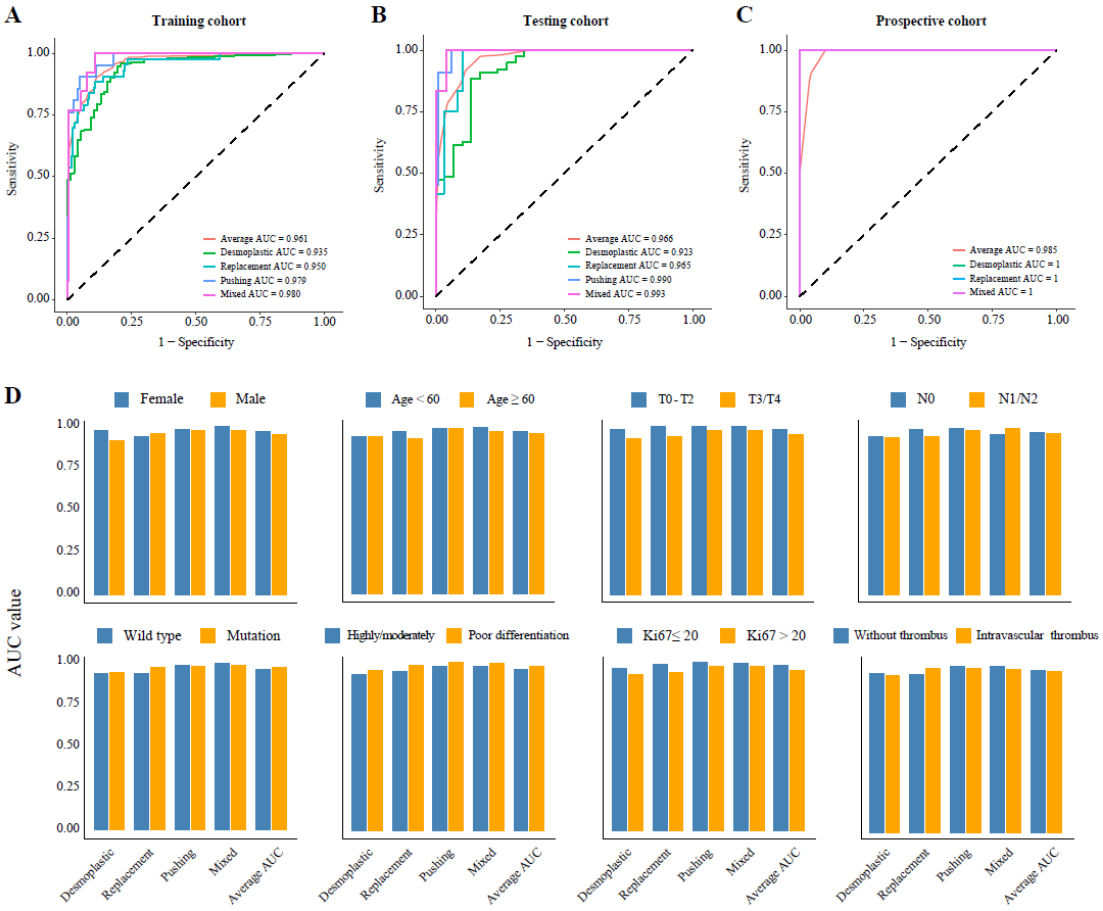

FIGURE 4. Four-class pathological classification prediction performance.
Performance in **A)** the training cohort, **B)** the testing cohort, and **C)** the prospective cohort, **D)** subgroup analysis of AUC values.

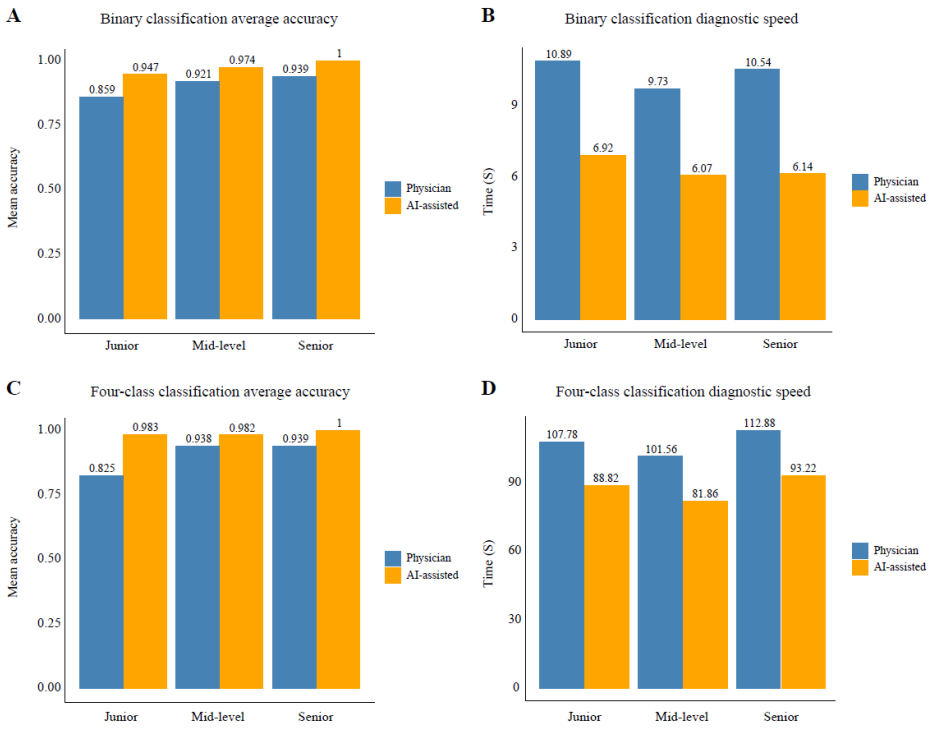

FIGURE 5. Impact of AI-assisted diagnostic performance in the prospective cohort. **A)** Binary classification diagnostic accuracy and **B)** diagnostic speed. **C)** Four-class diagnostic accuracy and **D)** diagnostic speed.

Received: 4 December, 2024
Accepted: 19 December, 2024
Published: 24 January, 2025

References

1. Rebecca L Siegel, Angela N Giaquinto, Ahmedin Jemal "Cancer statistics, 2024." *CA Cancer J Clin*, vol. 74, no, 1, pp. 12-49, 2024. Erratum in: *CA Cancer J Clin*, vol. 74, no. 2, pp. 203, 2024. View at: Publisher Site | PubMed
2. Ranmali Ranasinghe, Michael Mathai, Anthony Zulli "A synopsis of modern - day colorectal cancer: Where we stand." *Biochim Biophys Acta Rev Cancer*, vol. 1877, no. 2, pp. 188699, 2022. View at: Publisher Site | PubMed
3. René Adam, Aimery De Gramont, Joan Figueras, et al. "The oncosurgery approach to managing liver metastases from colorectal cancer: a multidisciplinary international consensus." *Oncologist*, vol. 17, no. 10, pp. 1225-1239, 2012. View at: Publisher Site | PubMed
4. L Viganò, B Branciforte, V Laurenti, et al. "The Histopathological Growth Pattern of Colorectal Liver Metastases Impacts Local Recurrence Risk and the Adequate Width of the Surgical Margin." *Ann Surg Oncol*, vol. 29, no. 9, pp. 5515-5524, 2022. View at: Publisher Site | PubMed
5. Pieter-Jan van Dam, Sofie Daelemans, Elizabeth Ross, et al. "Histopathological growth patterns as a candidate biomarker for immunomodulatory therapy." *Semin Cancer Biol*, vol. 52, no. Pt 2, pp. 86-93, 2018. View at: Publisher Site | PubMed
6. Florian E Buisman, Eric P van der Stok, Boris Galjart, et al. "Histopathological growth patterns as biomarker for adjuvant systemic chemotherapy in patients with resected colorectal liver metastases." *Clin Exp Metastasis*, vol. 37, no. 5, pp. 593-605, 2020. View at: Publisher Site | PubMed
7. Boris Galjart, Pieter M H Nierop, Eric P van der Stok, et al. "Angiogenic desmoplastic histopathological growth pattern as a prognostic marker of good outcome in patients with colorectal liver metastases." *Angiogenesis*, vol. 22, no. 2, pp. 355-368, 2019. View at: Publisher Site | PubMed
8. Wasswa William, Andrew Ware, Annabella Habinka Basaza-Ejiri, et al. "A pap-smear analysis tool (PAT) for detection of cervical cancer from pap-smear images." *Biomed Eng Online*, vol. 18, no. 1, pp. 16, 2019. View at: Publisher Site | PubMed
9. Ding-Qiao Wang, Long-Yu Feng, Jin-Guo Ye, et al. "Accelerating the integration of ChatGPT and other large-scale AI models into biomedical research and healthcare." *MedComm - Future Medicine*, vol. 2, no. 2, pp. e43, 2023. View at: Publisher Site
10. Dimitris Bertsimas, Georgios Antonios Margonis, Suleeporn Sujichantararat, et al. "Using Artificial Intelligence to Find the Optimal Margin Width in Hepatectomy for Colorectal Cancer Liver Metastases." *JAMA Surg*, vol. 157, no. 8, pp. e221819, 2022. View at: Publisher Site | PubMed

11. R Ferrari, C Mancini-Terracciano, C Voena, et al. "MR-based artificial intelligence model to assess response to therapy in locally advanced rectal cancer." *Eur J Radiol*, vol. 118, pp. 1-9, 2019. View at: Publisher Site | PubMed
12. Ming Y Lu, Bowen Chen, Drew F K Williamson, et al. "A visual-language foundation model for computational pathology." *Nat Med*, vol. 30, no. 3, pp. 863-874, 2024. View at: Publisher Site | PubMed
13. Ginimol Mathew, Riaz Agha, Joerg Albrecht, et al. "STROCSS 2021: Strengthening the Reporting of cohort, cross-sectional and case-control studies in Surgery." *Int J Surg*, vol. 96, pp. 106165, 2021. View at: Publisher Site | PubMed
14. Ming Y Lu, Drew F K Williamson, Tiffany Y Chen, et al. "Data-efficient and weakly supervised computational pathology on whole-slide images." *Nat Biomed Eng*, vol. 5, no. 6, pp. 555-570, 2021. View at: Publisher Site | PubMed
15. Alexey Dosovitskiy, Lucas Beyer, Alexander Kolesnikov, et al. "An image is worth 16x16 words: Transformers for image recognition at scale." *Computer Vision and Pattern Recognition*, 2020.
16. Julien Calderaro, Narmin Ghaffari Laleh, Qinghe Zeng, et al. "Deep learning-based phenotyping reclassifies combined hepatocellular-cholangiocarcinoma." *Nat Commun*, vol. 14, no. 1, pp. 8290, 2023. View at: Publisher Site | PubMed
17. Liu W, Lin Y, Liu Y, et al. "Vision Transformer for Small-Size Datasets." *Neurocomputing*, vol. 473, pp. 144-155, 2022.
18. Yunfang Yu, Wenhao Ouyang, Yunxi Huang, et al. "AI-Based multimodal Multi-tasks analysis reveals tumor molecular heterogeneity, predicts preoperative lymph node metastasis and prognosis in papillary thyroid carcinoma: A retrospective study." *Int J Surg*, 2024. View at: Publisher Site | PubMed
19. Mathilde Caron, Hugo Touvron, Ishan Misra, et al. "Emerging Properties in Self-Supervised Vision Transformers." *Proceedings of the IEEE/CVF International Conference on Computer Vision (ICCV)*, pp. 9650-9660, 2021.
20. Zhuchen Shao, Hao Bian, Yang Chen, et al. "TransMIL: Transformer based Correlated Multiple Instance Learning for Whole Slide Image Classification." *35th Conference on Neural Information Processing Systems (NeurIPS 2021)*.
21. Yunyang Xiong, Zhanpeng Zeng, Rudrasis Chakraborty, et al. "Nyströmformer: A nyström-based algorithm for approximating self-attention." *Proc AAAI Conf Artif Intell*, vol. 35, no. 16, pp. 14138-14148, 2021. View at: PubMed
22. Jie-Ying Liang, Shao-Yan Xi, Qiong Shao, et al. "Histopathological growth patterns correlate with the immunoscore in colorectal cancer liver metastasis patients after hepatectomy." *Cancer Immunol Immunother*, vol. 69, no. 12, pp. 2623-2634, 2020. View at: Publisher Site | PubMed
23. Diederik J Höppener, Pieter M H Nierop, Joost Hof, et al. "Enrichment of the tumour immune microenvironment in patients with desmoplastic colorectal liver metastasis." *Br J Cancer*, vol. 123, no.2, pp. 196-206, 2020. View at: Publisher Site | PubMed
24. Boris Galjart, Pieter M H Nierop, Eric P van der Stok, et al. "Angiogenic desmoplastic histopathological growth pattern as a prognostic marker of good outcome in patients with colorectal liver metastases." *Angiogenesis*, vol. 22, no. 2, pp. 355-368, 2019. View at: Publisher Site | PubMed
25. Pulathis N Siriwardana, Tu Vinh Luong, Jennifer Watkins, et al. "Biological and Prognostic Significance of the Morphological Types and Vascular Patterns in Colorectal Liver Metastases (CRLM): Looking Beyond the Tumor Margin." *Medicine (Baltimore)*, vol. 95, no. 8, pp. e2924, 2016. View at: Publisher Site | PubMed
26. Kåre Nielsen, Hans C Rolff, Rikke L Eefsen, et al. "The morphological growth patterns of colorectal liver metastases are prognostic for overall survival." *Mod Pathol*, vol. 27, no. 12, pp. 1641-1648, 2014. View at: Publisher Site | PubMed
27. Vitoria Ramos Jayme, Gilton Marques Fonseca, Isaac Massaud Amim Amaral, et al. "Infiltrative Tumor Borders in Colorectal Liver Metastasis: Should We Enlarge Margin Size?" *Ann Surg Oncol*, vol. 28, no. 12, pp. 7636-7646, 2021. View at: Publisher Site | PubMed
28. Pieter M H Nierop, Boris Galjart, Diederik J Höppener, et al. "Salvage treatment for recurrences after first resection of colorectal liver metastases: the impact of histopathological growth patterns." *Clin Exp Metastasis*, vol. 36, no. 2, pp. 109-118, 2019. View at: Publisher Site | PubMed
29. Hanna Nyström, Peter Naredi, Anette Berglund, et al. "Liver-metastatic potential of colorectal cancer is related to the stromal composition of the tumour." *Anticancer Res*, vol. 32, no. 12, pp. 5183-5191, 2012. View at: PubMed
30. Chiara Cremolini, Massimo Milione, Federica Marmorino, et al. "Differential histopathologic parameters in colorectal cancer liver metastases resected after triplets plus bevacizumab or cetuximab: a pooled analysis of five prospective trials." *Br J Cancer*, vol. 118, no. 7, pp. 955-965, 2018. View at: Publisher Site | PubMed
31. Zhaoyang Xu, Carlos Fernádez Moro, Danyil Kuznyecov, et al. "Tissue region growing for hispathology image segmentation." In: Proceedings of the 2018 3rd International Conference on Biomedical Imaging, Signal Processing. Bari, Italy: Association for Computing Machinery, 2018.
32. David Tellez, Diederik Höppener, Cornelis Verhoef, et al. "Extending unsupervised neural image compression with supervised multitask learning." *Proc Mach Learn Res*, vol. 121, pp. 770-783, 2020.
33. David Tellez, Geert Litjens, Jeroen van der Laak, et al. "Neural image compression for gigapixel histopathology image analysis." *IEEE Trans Pattern Anal Mach Intell*, vol. 43,no. 2, pp. 567-578, 2021. View at: Publisher Site | PubMed
34. Chiara Cremolini, Massimo Milione, Federica Marmorino, et al. "Differential histopathologic parameters in colorectal cancer liver metastases resected after triplets plus bevacizumab or cetuximab: a pooled analysis of five prospective trials." *Br J Cancer*, vol. 118, no. 7, pp. 955-965, 2018. View at: Publisher Site | PubMed
35. Artem Shmatko, Narmin Ghaffari Laleh, Moritz Gerstung "Artificial intelligence in histopathology: enhancing cancer research and clinical oncology." *Nat Cancer*, vol. 3, no. 9, pp. 1026-1038, 2022. View at: Publisher Site | PubMed